iPSC-Derived Trabecular Meshwork Cells Stimulate Endogenous TM Cell Division Through Gap Junction in a Mouse Model of Glaucoma

Shangru Sui,[1] Hongxia Yu,[1,2] Xiangji Wang,[1] Wenyan Wang,[1] Xuejiao Yang,[2] Xiaojing Pan,[3] Qingjun Zhou,[3] Chen Xin,[4] Rong Du,[4] Shen Wu,[4] Jingxue Zhang,[4] Qilong Cao,[5] Ningli Wang,[4] Markus H. Kuehn,[6,7] and Wei Zhu[1,8]

[1]Department of Pharmacology, School of Pharmacy, Qingdao University, Qingdao, China
[2]Affiliated Hospital of Qingdao University, Qingdao, China
[3]Qingdao Eye Hospital, Shandong Eye Institute, Shandong Academy of Medical Sciences, Qingdao, China
[4]Beijing Institute of Ophthalmology, Beijing Tongren Hospital Eye Center, Beijing, China
[5]Qingdao Haier Biotech Co. Ltd., Qingdao, China
[6]Department of Ophthalmology and Visual Sciences, University of Iowa, Iowa City, Iowa, USA
[7]Center for the Prevention and Treatment of Visual Loss, Iowa City Veterans Affairs Medical Center, Iowa City, Iowa, USA
[8]Beijing Advanced Innovation Center for Big Data-Based Precision Medicine, Beijing University & Capital Medical University, Beijing, China

Correspondence: Wei Zhu, Department of Pharmacology, School of Pharmacy, Qingdao University, Qingdao 266021, China; wzhu@qdu.edu.cn.

SS and HY contributed equally to this work.

PURPOSE. Decreased trabecular meshwork (TM) cellularity has been implicated as a major reason for TM dysfunction and aqueous humor (AH) outflow abnormalities in primary open angle glaucoma. We previously found that transplantation of induced pluripotent stem cell (iPSC)-derived TM cells can restore TM function and stimulate endogenous TM cell division. The goal of the present study is to investigate whether signaling via gap junctions is involved in this process.

METHODS. Differentiated iPSCs were characterized morphologically, transcriptionally, and immunohistochemically. After purification, iPSC-TM were co-cultured with mouse TM (MTM) cells to mimic the transplantation procedure. Through the pharmacological antagonists and short hairpin RNA (shRNA) technique, the gap junction function in iPSC-based therapy was determined.

RESULTS. In the co-culture system, iPSC-TM increase MTM cell division as well as transfer of Ca^{2+} to MTM. This effect was blocked by treatment with the gap junction inhibitors carbenoxolone (CBX) or flufenamic acid (FFA). The shRNA mediated knock down of connexin 43 (Cx43) expression in iPSC-TM also results in decreased Ca^{2+} transfer and lower MTM proliferation rates. In vivo, Cx43 downregulation in transplanted iPSC-TM weakened their regenerative role in an Ad5.myocilin^{Y437H} mouse model of glaucoma. Mice receiving these cells exhibited lower TM cellularity and higher intraocular pressure (IOP) than those receiving unmodified iPSC-TM.

CONCLUSIONS. Our findings reveal a crucial role of gap junction, especially Cx43, in iPSC-based TM regeneration, and provides insights to enhance the regenerative effect of iPSCs in glaucoma therapy.

Keywords: induced pluripotent stem cell (iPSC), trabecular meshwork (TM), regeneration, gap junction, intraocular pressure (IOP)

Sustained elevation of intraocular pressure (IOP) is the main reason for glaucoma, a degenerative optic neuropathy, and it is primarily caused by increased resistance to aqueous humor (AH) drainage.[1,2] In the conventional AH outflow, pathway resistance is mediated by the trabecular meshwork (TM) and the endothelial cells of Schlemm's canal.[3,4] Abnormalities of the TM resulting from a decrease in the cell population due to age or pathological reasons have been implicated in the development of elevated IOP in primary open angle glaucoma.[5] Several groups have demonstrated that stem cell-based therapy using adult TM stem

cells,[6,7] mesenchymal stem cells,[8] or induced pluripotent stem cells (iPSCs),[9] is a feasible approach to repopulate the damaged TM and maintain IOP homeostasis in the eye.

We previously described the influential role of iPSC-derived TM cells in the regeneration of the TM a mouse glaucoma model (Tg-MYOC^{Y437H}).[9,10] In these mice, TM damage results from the expression of a pathogenic variant of human myocilin.[11,12] Intracameral transplantation of iPSC-derived TM cells, referred to as iPSC-TM, can significantly lower the elevated IOP, increase AH outflow facility, and repopulate the damaged TM.[9] Transplantation of iPSC-TM can

also rebuild the senescent TM in human donor eyes with advanced age.[13] Interestingly, repopulation of the damaged TM appears to result from iPSC-TM mediated stimulation of endogenous TM cell division. This process requires cell-cell contact, but the molecular mechanism is still elusive.

Gap junction intercellular communication (GJIC) is a crucial biological process for neighboring cells to transfer ions, second messengers, and small molecules (less than 1.2 kD) from one to another to maintain tissue function, cellular growth, and proliferation.[14,15] In the eyes, gap junctions may allow ions and other survival regulators to spread from healthy cells to injured cells, thereby promoting cell survival.[16] Transferred molecules also include single-stranded RNA and gap junction mediated transfer of these from iPSC-derived bone marrow microvascular endothelial cells to neurons could improve the control of neurological diseases.[17,18] For example, it has been demonstrated that miR-200b moving through gap junction from bone marrow-derived mesenchymal stem cells to human umbilical vein endothelial cells influences osteogenesis.[19] We therefore wished to investigate whether gap junction plays a vital role in iPSC-TM induced stimulation of endogenous TM cell division.

To test our hypothesis, we first designed an in vitro coculture system and confirmed the capacity of iPSC-TM to stimulate TM cell proliferation. Exposure to the gap junction inhibitors or suppression of connexin 43 Cx43 expression by short hairpin RNA (shRNA) prevented the stimulating effect of iPSC-TM on TM cell division and significantly weakened the ability of iPSC-TM to lower elevated IOP in a mouse model of glaucoma.

MATERIALS AND METHODS

Animals

The 2-month-old male C57BL/6 mice were purchased from Beijing Vital River Laboratory Animal Technology Co., Ltd. (Beijing, China). Mice were housed under standard conditions with a 12 hour/12 hour day/night cycle (lights on at 7 AM and off at 7 PM), at 23 ± 2°C temperature and 50 ± 5% humidity. All experiments were conducted according to the ARVO Statement for the Use of Animals in Ophthalmic and Vision Research and the laboratory animal care and use guidelines of Qingdao University Medical Center.

TM Cells Isolation and Culture

Human TM (HTM) cells were derived from three donors obtained from the Iowa Lions Eye Bank (Iowa City, IA, USA). The protocol for human tissues collection was approved by the Eye Bank Association of America and was in accordance with the tenets of the Declaration of Helsinki. TM cells were maintained at Qingdao University in biopsy medium comprised of MEM-α basic medium (Gibco, Grand Island, NY, USA), 10% fetal bovine serum (FBS; Gibco), and 0.2% primocin (Invivogen, San Diego, CA, USA). TM cells at passage five to eight were characterized for the presence of TM biomarkers and elevated expression of myocilin following dexamethasone exposure prior to experimentation.[20,21]

Mouse TM (MTM) cells were isolated using a magnetic bead-based approach[22] that exploits the phagocytic activity of TM cells.[20] After sterilization in 75% alcohol, 2 µL magnetic microspheres (2.0 µm diameter, 25 mg/mL; Tianjin Baseline Chromtech Research Center, China) were injected into the anterior chamber of 2-week-old C57BL/6 mice using a Hamilton syringe (Hamilton Company, Reno, NV, USA) with a 30-gauge 0.5-inch sterile needle (Becton Dickinson, Franklin Lakes, NJ, USA). Mice receiving magnetic beads were euthanized on the second day after injection. After removing the iris and ciliary body, the iridocorneal tissues were digested in 1 × phosphate-buffered saline (PBS; Gibco) containing 4 mg/mL collagenase A (Sigma-Aldrich, St. Louis, MO, USA) and 4 mg/mL human serum albumin (Sigma-Aldrich). After purification through magnetic LD columns (Miltenyi Biotec, San Diego, CA, USA), cells were cultured in biopsy medium and placed in an incubator with 5% CO_2 at 37°C. MTM cells at passages 3 to 22, characterized following detection of TM biomarkers and Dex-induced myocilin expression,[20,21] were used in this study.

Mouse iPSCs

Mouse iPSCs, gifted by Professor Budd A. Tucker at the University of Iowa, were generated through reprogramming fibroblasts of 6-week-old dsRed expressing transgenic mice (B6.Cg-Tg(ACTB-DsRed*MST)1Nagy/J; Jackson Laboratory) by an ecotropic retrovirus carrying the Yamanaka factors (OSKM: Oct-3/4, Sox2, Klf4, and c-Myc). Successfully reprogrammed cells were transferred into plates coated with 0.2% matrigel (Becton Dickinson) and maintained in DEME/F12 medium (Gibco) comprised of 15% FBS (Gibco), 1% nonessential amino acids (NEAA; Gibco), 1% L-glutamine (Gibco), 0.2% Primocin (Invivogen), 0.0008% β-Mercaptoethanol (β-ME; Sigma-Aldrich), and 0.02% fresh mouse leukemia inhibitory factor (mLIF; Millipore, Danvers, MA, USA). Then, 0.1% ROCK inhibitor Y-27632 (Millipore) was added for iPSC seeding, passaging, or cryopreserving. Cells were cultured at 5% CO_2 and 37°C.

Mouse iPSC-TM Differentiation and Purification

Cell culture medium conditioned by HTM cultures derived from the three donors was collected and pooled. After sterilization by filtration through mixed cellulose ester membrane filters (0.2 µm pore size; Millipore) the conditioned medium was applied to induce mouse iPSCs differentiation for 10 days.

Differentiated cells derived from iPSCs were purified by a magnetic bead-based approach that exploits the SSEA-1 expression of undifferentiated cells. The 1,000,000 mixed cells were incubated with 100 µL of a 20% (wt/vol) solution of PE Mouse anti-SSEA-1 (Becton Dickinson) for 20 minutes at 4°C. Cells were collected by centrifugation and resuspended in 80 µL 1 × PBS (Gibco) buffer containing 0.5% bovine serum albumin (BSA; Sigma-Aldrich) and 2 mM ethylene diamine tetraacetic acid (EDTA; Sigma-Aldrich). Undifferentiated cells were labeled with anti-PE microbeads and removed through LD columns placed in a magnetic field (Miltenyi Biotec). Purified cells are referred to as iPSC-TM.

Flow Cytometry Analysis

Successful removal of undifferentiated iPSC was confirmed by fluorescence-activated single cell sorting (FACS). The 1,000,000 purified cells were rinsed with 1 × PBS (Gibco) and suspended in 1 × PBS buffer containing 1% FBS (Gibco). After incubation with PE-conjugated mouse anti-SSEA-1 antibodies (1:5, Becton Dickinson, 560142) for 30 minutes at 4°C, the cells were rinsed and resuspended in 500 µL buffer

as described above for FACS. The PE-positive cell ratio was determined using BD FACSCalibur (Becton Dickinson). Unstained cells were used as a negative control. The voltage and amp gain of the forward scatter (FSC) was E00 and 1.00, and that of the side scatter (SSC) was 340 and 1.00. The voltage of fluorescence2 (FL2) was 381.

Coculture Experiment

MTM cells were incubated with 5 µM CellTracker Red CMTPX (Invitrogen, Carlsbad, CA, USA, C34552) for 20 minutes at 37°C. A stock solution of CellTracker Red CMTPX (Invitrogen; 10 mM) was made in DMSO (Sigma-Aldrich) and stored at −20°C. The working solution of CellTracker Red CMTPX (Invitrogen, 5 µM) was prepared by diluting the stock solution into the medium. The 3000 MTM cells were seeded on a borosilicate glass-bottom cell culture dish with 15 mm diameter (NEST, Wuxi, China). After culture for 6 hours, 1500 iPSC-TM cells (without fluorescent label) were collected and seeded to the same dish. After coculture for 24 or 48 hours, the cells were fixed in 4% paraformaldehyde (Thermo, Waltham, MA, USA) for 20 minutes at room temperature. Cell nuclei were stained with 4, 6-diamidino-2-phenylindole (DAPI; Santa Cruz Biotechnology, Inc., Dallas, TX, USA). The stained cells were imaged at 40× magnification by confocal microscopy (Nikon A1MP multiphoton confocal microscope; Nikon, Tokyo, Japan) and counted manually by one of the investigators (S. Sui). Quantification of cells with red fluorescence, considered to be MTM cells, occurred in a double-blinded fashion.

5-Bromo-2′-Deoxyuridine Incorporation Assay

A 10 mM 5-bromo-2′-deoxyuridine (BrdU) stock solution was prepared in DMSO and diluted in HTM culture medium to a final concentration of 10 µM. Cells were incubated with BrdU at 37°C for 2 hours. Cells were then washed with 1 × PBS (Gibco), fixed in 4% paraformaldehyde (Thermo) for 30 minutes, treated with 0.3% Triton X-100 (Sigma-Aldrich) for 5 minutes, incubated with anti-BrdU primary antibody (1:100; Thermo; MA3-071) overnight, and labeled with a secondary antibody (Alexa Fluor 488 goat anti-mouse immunoglobulin G; Invitrogen). Samples were mounted using an anti-fluorescence quenching agent (Solarbio, Beijing, China) and imaged by confocal microscopy (Nikon).

Inhibitor Treatment

Stock solution of CBX (100 mM) and FFA (100 mM) were made in DMSO (Sigma-Aldrich) and stored at 4°C. Working solutions of CBX (50 µM) and FFA (50 µM) were prepared by diluting the stock solution into the medium. MTM and iPSC-TM cells in the coculture system were exposed to 50 µM CBX (Sigma-Aldrich; C4790) or 50 µM FFA (Abcam, Cambridge, MA, USA; ab120354). 0.05% (wt/vol) DMSO (Sigma-Aldrich) was used as the vehicle control.

Intracellular Calcium Concentration Analysis

Green fluorescent calcium-binding dye (Fluo-8 AM; 4 µM; Abcam; ab142773) was added to the coculture system and incubated for 1 hour at 37°C. Cells were rinsed with 1 × PBS (Gibco) and imaged at 100× magnification by confocal microscopy (Nikon). All images were taken using the same microscope settings allowing quantification of intracellular

calcium concentration indicated by green fluorescence. The, two to three areas in each slide were imaged, and the average from three slides was taken as calcium concentration in each group. Values are reported as arbitrary fluorescence units.

Calcium Transfer Analysis

Purified iPSC-TM cells were stained with 4 µM Fluo-8 AM (Abcam) for 1 hour at 37°C. MTM cells were stained with CellTracker Red CMTPX (Invitrogen) as described above. The iPSC-TM and MTM cells were rinsed with 1 × PBS (Gibco) and seeded on borosilicate glass-bottom cell culture dish (NEST). After a 20-minute incubation, cells were imaged by confocal microscopy (Nikon). Green fluorescence in MTM cells was considered as an indication of transfer of calcium conjugated to Fluo-8 from iPSC-TM cells.

Cell Counting Kit-8 Assay

Cell viability was assessed through the Cell Counting Kit-8 (CCK-8; Boster, Wuhan, China). Then, 1000 cells were seeded into each well of a 96-well plate (Thermo) and cultured in an incubator with 5% CO_2 at 37°C for 6 hours. CCK-8 solution (1:10) was added and cells were incubated for 2 hours at 37°C in the dark. The absorbance (A) at 450 nm wavelength was determined in each well by a microplate reader (SpectraMax L; Molecular Devices, San Jose, CA, USA). The data presented represent the averages of 6 replicates using MTM cells from 20 eyes or purified iPSC-TM cells.

Preparation of Lentivirus

Cx43 shRNA and scrambled shRNA oligonucleotides (Table 1) were cloned into the pHBLV-U6-MCS-CMV-ZsGreen-PGK-PURO plasmid vector (Shanghai Hanbio Technology Co., Ltd, Shanghai, China). Plasmids carrying either shRNA Cx43 or scrambled shRNA, psPAX2, and pMD2G vectors were cotransfected into HEK293 cells using LipoFiter transfection reagents to generate the recombinant virus (Shanghai Hanbio Technology). The titer was measured using a standard plaque assay. Stock solutions of lentivirus containing 2 × 10⁸ transducing units (TUs)/mL were prepared.

Lentiviral Infection

The 300,000 iPSC-TM cells were infected with recombinant lentivirus carrying Cx43 shRNA or scrambled shRNA at multiplicity of infection (MOI) of 5[23] for 26 hours at 37°C. Cells were maintained in biopsy medium for 6 days before collection for real-time PCR (RT-PCR), Western blot analysis, and coculture experiment.

Infection of Adenovirus 5

Recombinant adenovirus 5 (Ad5)-MYOC[Y437H]-EGFP[24] and Ad5-EGFP were gifted by Beijing Tongren Hospital (Beijing, China). Mutant MYOC[Y437H] was created by site directed mutagenesis of T 1309 to C of human *Myocilin* and these constructs were cloned into an adenovirus plasmid (pBHGlox E1, 3). The plasmids of pDC311 and pBHGlox E1, 3 Myoc[Y437H] were cotransfected into HEK293 cells to generate the recombinant adenovirus 5, referred to as Ad5-MYOC[Y437H]-EGFP, using LipoFiter transfection reagent (Shanghai Hanbio Technology Co., Ltd) to generate the recombinant virus. Ad5 virus expressing only EGFP, referred

TABLE 1. Sequences of Scrambled shRNA and Cx43 shRNA

Scrambled shRNA sequence:
GATCCGTTCTCCGAACGTGTCACGTAATTCAAGAGATTACGTGACACGTTCGGAGAATTTTTTC
Cx43 shRNA sequence:
GATCCGAACCTACATCATCAGTATTTCAAGAGAATACTGATGATGTAGGTTCTTTTTTG

to as Ad5-EGFP, was used as a control. Ad5 stocks containing 3.2×10^{10} plaque formation unit (PFU)/mL were prepared and stored at $-80°C$. The 100,000 MTM cells were then infected with Ad5-MYOC^{Y437H}-EGFP virus or Ad5-GFP at 200 MOI[25] for 8 hours. Cells were maintained in biopsy medium for 6 days before collection for TdT-mediated dUTP Nick-End Labeling (TUNEL) analysis.

Western Blotting

Proteins were extracted with RIPA buffer containing Halt Protease Inhibitor Cocktail (Thermo) and quantified with BCA protein analysis kit (Thermo). Then, 40 µg proteins were boiled for 5 minutes and separated on a 10% sodium dodecyl sulfate (SDS)-acrylamide gel by electrophoresis. Proteins were transferred to a polyvinyl difluoride membrane (PVDF; GE Healthcare Life Sciences China, Beijing, China) by Mini Trans-Blot Cell (Bio-Rad) at 150 mA current for 2 hours. The membrane was then incubated in a blocking buffer (Tris-buffered Saline-Tween-20 [TBST] containing 5% non-fat milk powder) at room temperature for 1.5 hours. After incubation with the diluted rabbit polyclonal Cx43 (1:6000; Abcam; ab11370) or rabbit polyclonal GAPDH (1:10000; Abcam; ab181602) overnight at 4°C, membranes were rinsed with TBST three times and incubated with the secondary antibody conjugated to horseradish peroxidase (HRP; Abcam) at room temperature for 1 hour. Immunoreactive bands were visualized using the enhanced chemiluminescence detection kit (Thermo) and a ChemiDoc XRS^{+} imaging system (Bio-Rad). Band intensity of Cx43 was quantified using Image Lab software (Bio-Rad) and normalized to GAPDH. Experiments were carried out in triplicate.

Real-Time PCR

Total RNA was extracted using TRIzol reagent (Ambion, Inc., Austin, TX, USA) and quantified using a Nano-photometer (Implen, Munich, Germany). RNA samples with ratios of optical density at 260 and 280 nm between 1.8 and 2.1 were used. The cDNA was generated using a random primed reverse transcription reaction (TIANGEN, Beijing, China). The samples were amplified in triplicate using SYBR Green reagents (Bio-Rad, Hercules, CA, USA) and primers designed by Primer3 (http://primer3.ut.ee; Table 2). PCR reaction conditions were: 95°C for 15 minutes, then 50 cycles at 95°C for 10 seconds, 50°C for 30 seconds, and 72°C for 30 seconds. Specific amplification of the primers was confirmed by melt curve analysis. *β-Actin* and GAPDH were used as reference genes. A comparative cycle threshold method was used for data analysis.[26]

TUNEL Analysis

Cells were fixed in 4% paraformaldehyde (Thermo) for 30 minutes, treated with 0.3% Triton X-100 (Sigma-Aldrich) for 5 minutes, and incubated with 50 µL of TUNEL mixture containing 5 µL TdT enzyme and 45 µL fluorescence detection solution (Beyotime, Shanghai, China) for 60 minutes at 37°C. Cell nuclei were stained with DAPI (Santa Cruz). The samples were mounted using an anti-fluorescence quenching agent (Solarbio, Beijing, China) and imaged by confocal microscopy, as described above. Apoptotic cells become red fluorescence-positive and were quantified using 10× magnification images. Experiments were carried out in triplicate using MTM cells from 20 eyes.

Intracameral Injection

Mice were subjected to deep anesthesia using 8% chloral hydrate (0.125 mL/20 g). Ad5-MYOC^{Y437H}-EGFP (8×10^7 PFU; 2.5 µl)[27] was intracamerally injected into one eye of 2 month old C57BL/6 mice using a Hamilton syringe connected to a sterile needle (30-gauge, 1/2-inch length; Becton Dickenson). The contralateral eye received the same amount of Ad5-EGFP. In the cell transplantation experiment, 50,000 iPSC-TM cells transfected with either Cx43 shRNA or scrambled shRNA were resuspended in 3 µL $1 \times$ PBS (Gibco) and injected into the anterior chamber. Mice having received an equal amount of $1 \times$ PBS (Gibco) were used as the control. Mice were kept on a heated blanket at 37°C until they recovered from the surgery.

IOP Measurement

Mice were anesthetized with 2.5% isoflurane and 80% (vol/vol) oxygen (RWD Life Science Co., Ltd., Shenzhen, China) for 5 minutes. IOP was measured by rebound tonometry (TonoLab, Helsinki, Finland), as previously described.[9] Measurements were taken between 9:00 AM and 12:00 AM, and data represent the average of 3 measurements.

TABLE 2. The Primers for RT-PCR Analysis

Gene	Forward Primer (5′ to 3′)	Reverse Primer (5′ to 3′)
mSOX2	TGATGGAGACGGAGCTGAAG	GCTTGCTGATCTCCGAGTTG
mTIMP3	CCCTTTGGCACTCTGGTCTA	CCACCTCTCCACAAAGTTGC
mNanog	ATGCGGACTGTGTTCTCTCA	TGCTGAGCCCTTCTGAATCA
Cx43	TGTGGACATGCACTTGAAGC	TGTGGGCAGGGATCTCTTTT
GAPDH	GGGTCCCAGCTTAGGTTCAT	CATTCTCGGCCTTGACTGTG
β-Actin	CATTGCTGACAGGATGCAGAAGG	TGCTGGAAGGTGGACAGTGAGG

Preparation of Cryosections

Enucleated mouse eyes were pierced using a 30-gauge syringe needle (Becton Dickenson) and fixed immediately by immersion in 4% paraformaldehyde (Thermo) for 2 hours at room temperature. After rinsing with $1 \times$ PBS (Gibco) and infiltration with 13.3%, 15.0%, and 16.7% (wt/vol) of sucrose solutions, the tissues were embedded in optimal cutting temperature compound (OCT; Sakura, Tokyo, Japan) and sectioned to 10 μm thickness on a Leica CM1950 cryostat (Leica, Nussloch, Germany).

Immunohistochemical Staining

Samples, including cell culture samples and cryosectioned tissues, were rinsed with $1 \times$ PBS (Gibco) and treated with 0.3% Triton X-100 (Sigma-Aldrich) to increase permeability. After incubation in blocking buffer comprised of $1 \times$ PBS (Gibco), 1% BSA (Sigma-Aldrich), and 0.3% Triton X-100 (Sigma-Aldrich) for 1 hour, samples were incubated with the diluted primary antibodies (1:100) followed by the corresponding secondary antibodies (1:200). Cell nuclei were stained with DAPI (Santa Cruz). Samples were mounted using an anti-fluorescence quenching agent (Solarbio, Beijing, China) and imaged by confocal microscopy (Nikon).

The primary antibodies include rabbit polyclonal anti-RFP (Abcam, ab185921), rabbit polyclonal anti-Cx43 (Abcam, ab11370), rabbit polyclonal anti-TIMP3 (Abcam, ab39184), rabbit polyclonal anti-SOX2 (Abcam, ab97959), rabbit monoclonal anti-Nanog (Abcam, ab109250), and rabbit polyclonal anti-LAMA4 (Abcam, ab209675). The secondary antibody was Alexa Fluor 568 goat anti-rabbit immunoglobulin G (IgG; Invitrogen).

TM Cellularity Analysis In Vivo

For quantification of iPSC-TM cells in the TM high-magnification images ($40\times$) of the TM and Schlemm's canal were used. In each image, cells localized in the region between the pigmented ciliary body and Schlemm's canal were counted. Each group contained four to five eyes and five cryosections from each eye were analyzed. The average of these 20 to 25 counts was taken as TM cellularity of the group. The number of endogenous TM cells was calculated by subtracting the number of transplanted iPSC-TM cells identifiable by red fluorescence from the total number of TM cells.

Statistical Analysis

The Shapiro-Wilk test was used to test for normality. A two-tailed *t*-test was applied for statistical analysis of the IOP data. One-way ANOVA was performed for statistical analysis of the cellularity and intracellular calcium concentration. All tests were performed in GraphPad Prism 7 and data are expressed as the mean $\pm$ SEM. The *P* values < 0.05 were considered to be statistically significant.

RESULTS

Mouse iPSC-TM Stimulate MTM Division In Vitro

For this experiment, MTMs were obtained using a magnetic bead-based approach and characterized based upon their cell morphology, biomarker expression, and dexamethasone-inducible myocilin expression[28,29] (Fig. 1A). Furthermore, we induced mouse iPSCs to differentiate into a TM-like cell type, designated iPSC-TM, using tissue culture medium conditioned by three verified HTM cultures, as previously described.[9,28] After approximately 3 to 5 days, cells around the iPSC colonies begin to exhibit TM cell-like morphology typified by their spindle-like shape, although at this stage iPSC-TM cells are smaller than MTM cells.[13,20] Continuous culture in conditioned medium causes these cells to increase in size until they reach a size similar to that of MTM cells (see Fig. 1A). We also determined whether differentiated iPSCs exhibit TM features by RT-PCR (Fig. 1B) and immunohistochemistry (IHC, Fig. 1C).[9,20] RT-PCR results show that differentiation causes an increase of tissue inhibitor of matrix proteases 3 (TIMP3) expression, but a downregulation of two stem cell biomarkers: Nanog homeobox (Nanog) and SRY box 2 (Sox2; see Fig. 1B). Purified iPSC-TM were also used for IHC analysis (see Fig. 1C). Unlike iPSCs, iPSC-TM cells exhibit immunoreactivity to TIMP3 and laminin $\alpha4$ (LAMA4) antibodies and do not react with either Nanog or Sox2 antibodies, in accordance with expression patterns observed in MTM (see Fig. 1C).

In our previous investigations, we noted that survival of transplanted iPSC-TM cells in the eye is low despite their ability to regenerate the TM. This suggested that functional restoration is due to repopulation of the TM with endogenous cells.[9,10,13,30] To further examine this phenomenon, we developed an in vitro coculture system and tested whether purified iPSC-TM cells have the capacity to stimulate MTM cell division and whether stimulation is dependent upon Gap junction mediated cell-cell communication.

MTM cells were labeled with CellTracker Red CMTPX and then cocultured with iPSC-TM for 24 or 48 hours (Fig. 1D). Quantification of MTM demonstrated that their cellularity significantly increased after coculture when compared to the control (24 hours: 2636.0 ± 24.7 vs. 2314.0 ± 87.6 cells/dish, $P = 0.02$; 48 hours: 3776.0 ± 153.3 vs. 3202.0 ± 79.9 cells/dish, $P = 0.03$). Of note, we did not observe transfer of CellTracker from the prelabeled MTM into iPSC-TM cells (Supplementary Fig. S1). The ability of iPSC-TM to cause mitosis in TM cells was further confirmed in a BrdU incorporation assay (Supplementary Fig. S6). Moreover, we found that the ability of iPSC-TM cells to stimulate the cell division of MTM cells is dependent upon the passage number of these primary cultures (Supplementary Fig. S2). Whereas MTM cells at passage 17 (P17) increased by $42.8 \pm 10.4\%$ ($P = 0.0008$) those at passage 22 (P22) increased only by $11.0 \pm 3.4\%$ ($P = 0.01$).

Gap Junction Antagonists Inhibit iPSC-TM Stimulating MTM Cell Division

Data reported by our and other laboratories indicate that the stimulation of TM cell division induced by either iPSC-TM or TM stem cells is not a paracrine effect, but requires cell-cell contact.[13,31] Because gap junctions mediate communication between neighboring cells in a variety of tissues,[21] we sought to investigate their role in the functional regeneration of the glaucomatous TM. Two selective gap junction antagonists, CBX or FFA, were applied in the coculture system to investigate if iPSC-TM cells stimulate MTM cell division through these channels. To avoid confounding effects of drug toxi-
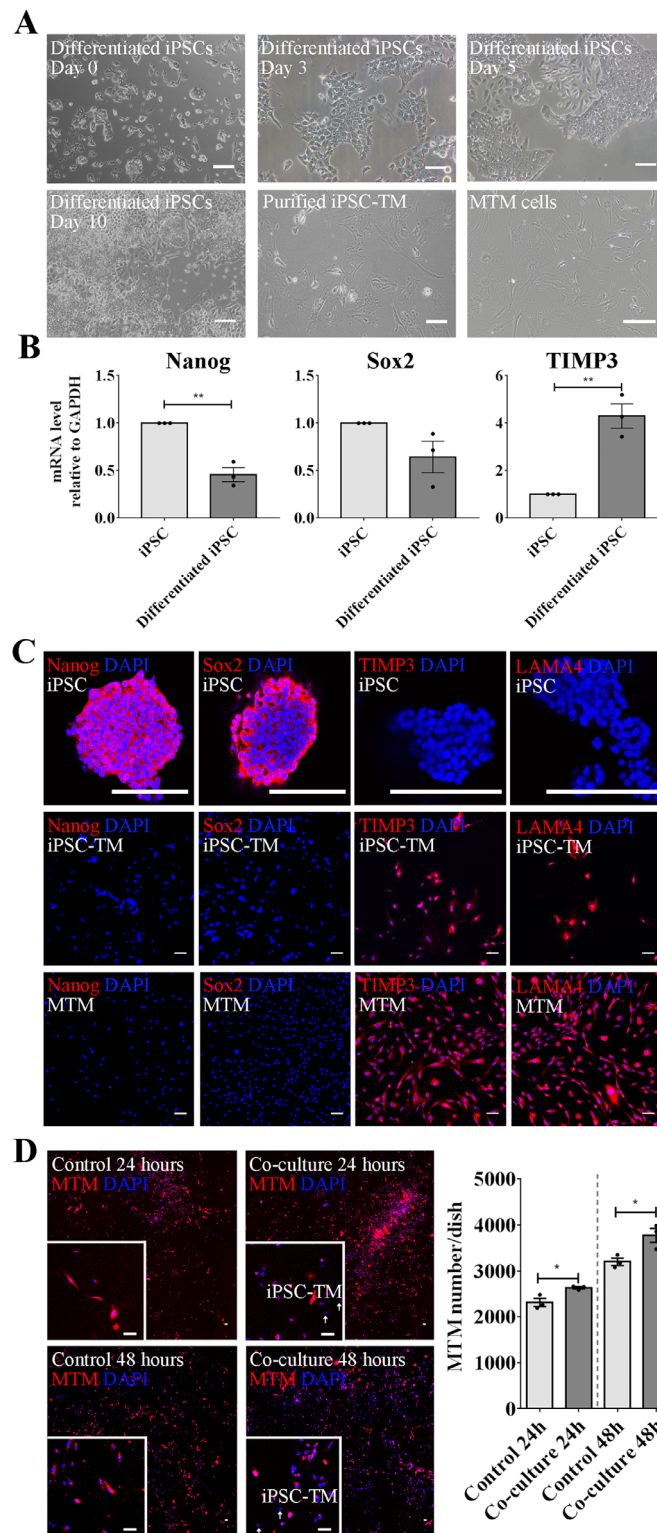
FIGURE 1. Coculture with iPSC-TM stimulates MTM cell division. (**A**) Morphology of undifferentiated iPSCs (day 0), iPSC-TM after differentiation for 3, 5, 10 days, as well as purified iPSC-TM and MTM cells. In comparison with iPSC colonies, differentiated cells display a spindle-like shape similar to MTM cells and exhibit TM features, including expression of TM biomarkers and dexamethasone-inducible myocilin expression. (**B**) Relative mRNA levels of Nanog and Sox2 are higher in undifferentiated iPSC than in those differentiated for 10 days, whereas TIMP3 showed a significantly higher expression in the differentiated cells ($n = 3$). GAPDH was used as the reference gene. (**C**) Immunohistochemical staining of Sox2 (*red*), Nanog (*red*), TIMP3 (*red*), and LAMA4 (*red*) in undifferentiated iPSC, iPSC-TM, and MTM. Nuclei are labeled with DAPI (*blue*). Typical results from $n = 3$ technical repeats are shown. (**D**) *Left panel*: The 40× magnification images of MTM cells labeled with CellTracker Red CMTPX cocultured with iPSC-TM for 24 and 48 hours. Nuclei are labeled with DAPI (*blue*). The region in the white frame shows a magnified view. Typical results from $n = 3$ technical repeats are shown. *Right panel*: Quantification of MTM cells (*red*) in the control and cocultured groups after 24 and 48 hours. Purified iPSC-TM cells significantly stimulate MTM division, both after 24 hours and 48 hours coculture. *$P < 0.05$, **$P < 0.01$ by two-tailed t-test. Scale bar = 100 μm. Data shown represent means ± SEM.

city, we first confirmed cell viability after treatment with CBX or FFA at the target concentration (50 µM for each inhibitor; Supplementary Fig. S3). Data obtained by CCK8 analysis revealed that neither CBX nor FFA treatment exhibit a toxic effect on iPSC-TM or MTM at this concentration. Drug treatments not only prohibit gap junction function, but also cause downregulation of the Cx43 expression, which further weakens the capacity of iPSC-TM to stimulate MTM division (Supplementary Fig. S4).[32–36] Although the number of MTM cells in control cultures increased to 2636.0 ± 24.7 cells/dish after 24 hours of coculture, those maintained in the presence of CBX or FFA exhibited significantly reduced proliferation (2469.0 ± 53.1 and 2267.0 ± 118, $P = 0.30$ and 0.03, respectively). This effect became more pronounced after 48 hours of coculture when control cell numbers increased to 3776.0 ± 153.3 cells/dish, whereas CBX or FFA treated cultures continued to display lower cell numbers (3161.0 ± 83.5 and 3117.0 ± 38.7 cells/dish, respectively; $P = 0.01$ for both conditions; Fig. 2A). These results suggest that the capacity of iPSC-TM to stimulate MTM division is dependent on gap junctions.

iPSC-TM Stimulate an Increase of Calcium Levels in MTM

Calcium plays a crucial role in regulating cell division and is readily transferred between cells through gap junction channels. In order to explore whether Ca^{2+} transfer from iPSC-TM to MTM contributes to increased cell division, we designed a Ca^{2+} transfer experiment. MTM cells were labeled with CellTracker Red CMTPX (red), whereas iPSC-TM cells were stained with a Ca^{2+} sensitive dye, Fluo-8 AM (green). After coculture for 20 minutes green fluorescence, indicative of Ca^{2+} conjugated to Fluo-8, can be observed in red MTM cells, suggesting a transfer of Ca^{2+} from iPSC-TM to MTM cells (Fig. 2B). We further quantified the fluorescence intensities (in arbitrary units) of Fluo-8 in individual iPSC-TM and iPSC-TM cells connected to MTM cells. As shown in Figure 2B, a significant decrease of Fluo-8 intensity can be observed in iPSC-TM interacting with MTM cells (183.8 ± 6.6 vs. 209.2 ± 6.1, $P = 0.007$, $n = 20$ cells). Moreover, we quantified Ca^{2+} transfer by analyzing intercellular calcium concentration, designated $[Ca^{2+}]_i$, in MTM cells. After co-culture with iPSC-TM for 24, 48, and 72 hours, $[Ca^{2+}]_i$ in MTM is significantly elevated when compared with controls (24 hours: 955.2 ± 58.8 vs. 644.9 ± 27.9, $P < 0.0001$; 48 hours: 1330.0 ± 70.7 vs. 640.2 ± 58.4, $P < 0.0001$; 72 hours: 830.6 ± 58.7 vs. 640.3 ± 38.9, $P = 0.01$; Fig. 2C). The increase can be diminished by treatment with either CBX (50 µM; 24 hours: 1167.0 ± 91.7 vs. 620.2 ± 60.9, $P = 0.01$; 48 hours: 985.2 ± 68.3 vs. 543.6 ± 43.2, $P < 0.01$) or FFA (50 µM; 24 hours: 1167.0 ± 91.7 vs. 806.3 ± 100.4, $P = 0.06$; 48 hours: 985.2 ± 68.3 vs. 813.8 ± 53.4, $P = 0.16$; Figs. 2D, 2E). In contrast, fluorescence intensity of Fluo-8 in the cocultured iPSC-TM showed no significant change resulting from treatment with either CBX (50 µM; 24 hours: 973.1 ± 56.9 vs. 1045.0 ± 38.7, $P = 0.8$; 48 hours: 993.6 ± 48.0 vs. 949.7 ± 101.4, $P = 0.9$) or FFA (50 µM; 24 hours: 1001.0 ± 132.9 vs. 1045.0 ± 38.7, $P = 0.9$; 48 hours: 993.6 ± 48.0 vs. 879.2 ± 60.9, $P = 0.5$) when compared to the DMSO treated control group (see Fig. 2E). Taken together, these findings indicate that during coculture gap junction mediated transfer of Ca^{2+} occurs from iPSC-TM to MTM cells.

Cx43 shRNA Inhibits iPSC-TM Stimulation of MTM Cell Division

Both CBX and FFA inhibit gap junction channels comprised of various subunits and accordingly do not provide an indication which gap junction protein(s) may be involved. Cx43 is the most abundant protein of the gap junction family in the TM and serves important functions in the regulation of AH outflow and IOP homeostasis.[21,37] We thus explored the role of Cx43 in the iPSC-TM-induced stimulation of MTM division. IHC analysis demonstrated not only that Cx43 is expressed on both individual iPSC-TM or MTM cells, but it can also be found at the junction between iPSC-TM and MTM cells (Fig. 3A). We then downregulated Cx43 expression in iPSC-TM through shRNA mediated knock down. Purified iPSC-TM cells were infected with lentivirus expressing either Cx43 shRNA and EGFP or scrambled shRNA and EGFP. The inclusion of the EGFP tag allows estimation of infection efficiency by IHC and revealed similar infection efficiencies between the CX43 shRNA vector ($56.0 \pm 2.9\%$) and the scrambled control ($59.6 \pm 5.0\%$; Figs. 3B, 3C). Transfection of iPSC-TM results in a significant decrease of detectable Cx43 mRNA as determined by RT-PCR ($61.6 \pm 2.6\%$, $P < 0.0001$; Fig. 3D) and protein level as determined by Western blot ($50.0 \pm 2.2\%$, $P < 0.0001$; Fig. 3E). As hypothesized, these modified iPSC-TM cells do not stimulate MTM cell division as efficient as normal iPSC-TM (3001.0 ± 137.6 vs. 2640.0 ± 153.9 cells/dish, $P = 0.01$; Fig. 3F). To confirm the role of Cx43 in calcium transfer, we cocultured MTM prestained with Cell-Tracker Red CMTPX and iPSC-TM infected with lentivirus carrying Cx43 shRNA-EGFP for 48 hours, and stained them with Fluo-8 AM for 1 hour. In comparison to the effect of normal iPSC-TM on calcium influx into MTM, downregulation of Cx43 results in a slightly lower increase of intracellular calcium levels in MTM (Fig. 3G). However, findings did not reach statistical significance (0.8 ± 0.2 vs. 1.0 ± 0.2, $P = 0.5$, $n = 8$).

Expression of MYOC[Y437H] Leads to Loss of TM Cells

We next aimed to explore whether interference with Cx43 expression influences the regenerative capacity of iPSC-TM in vivo. For these experiments, we exploited the ability of a pathogenic variant of myocilin, MYOC[Y437H], to cause TM cell death and IOP elevation.[24] Quantification of apoptotic cells, as revealed by TUNEL assay, demonstrated that infection of cultured MTM with Ad5-MYOC[Y437H]-EGFP causes a significant increase of apoptotic cells when compared with cultures infected with Ad5-EGFP ($24.7 \pm 6.4\%$ vs. $0.2 \pm 0.2\%$, $P = 0.02$; Fig. 4A).

This phenomenon was not only observed in vitro, but also detected in vivo. Ad5-MYOC[Y437H]-EGFP (8×10^7 PFU) was injected unilaterally into the anterior chamber of 2 month old C57BL/6 mice while the contralateral eye received the same amount of Ad5-EGFP ($n = 17$). Eyes of wild type (WT) mice received a PBS injection and were used as the controls ($n = 6$). IHC demonstrated robust expression of EGFP in Ad5-MYOC[Y437H]-EGFP treated eye, suggesting strong MYOC[Y437H] expression in the TM (left panels in Fig. 4B). As observed in vitro, MYOC[Y437H] expression caused a dramatic decrease of MTM cellularity in vivo (2 weeks: 27.4 ± 2.0 vs. 35.4 ± 2.3 cells/section, $P = 0.04$, $n = 4$; 4 weeks: 23.3 ± 2.5 vs. 37.8 ± 3.2 cells/section, $P = 0.01$, $n = 5$; 8 weeks: 24.7 ± 1.0 vs. 40.8 ± 2.7 cells/section,
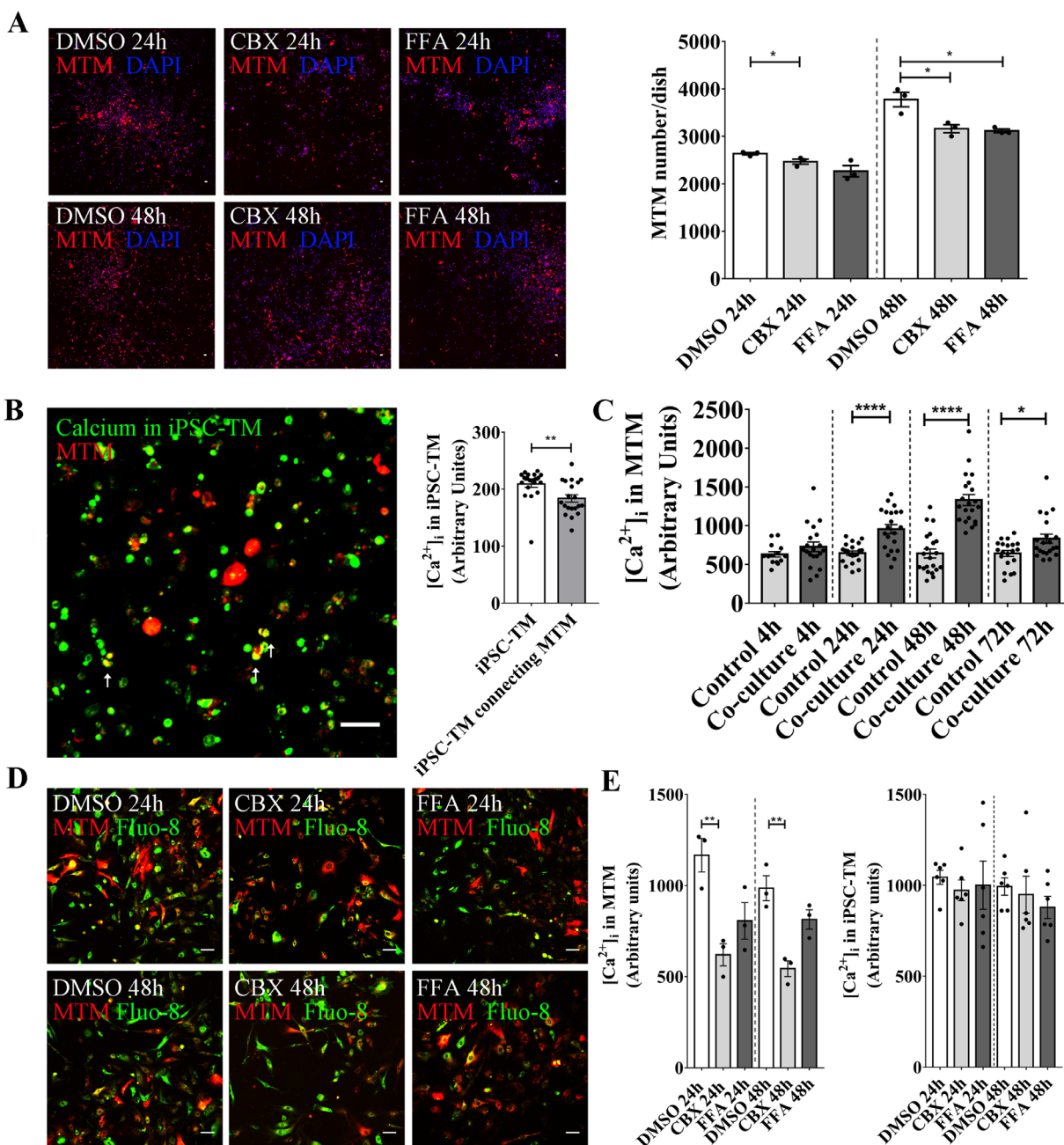
FIGURE 2. **CBX and FFA prevent iPSC-TM stimulation of MTM cell division.** (**A**) *Left panel*: Histochemical staining of MTM cells pre-labeled with CellTracker Red CMTPX after coculture with iPSC-TM for 24 and 48 hours, in the presence or absence of the gap junction antagonists CBX or FFA. DMSO was used as the vehicle control. Nuclei are labeled with DAPI (*blue*). Typical results from $n = 3$ technical repeats are shown. *Right panel*: Quantification of MTM cells (*red*) in the co-cultured group treated with DMSO, CBX, or FFA for 24 and 48 hours. CBX or FFA treatment significantly reduce iPSC-TM stimulation of MTM division after 24 and 48 hours of co-culture. *$P < 0.05$ by one-way ANOVA. (**B**) *Left panel*: Ca^{2+} conjugated with Fluo-8 (*green*) transfer from iPSC-TM to MTM pre-labeled with CellTracker Red CMTPX (*red*). *Right panel*: Quantitative analysis of $[Ca^{2+}]_i$ indicating a significant decrease of Fluo-8 intensity in iPSC-TM after interacting with MTM cells. (**C**) Quantification of green fluorescence intensity shows that intercellular calcium concentration, $[Ca^{2+}]_i$, in MTM cells is significantly increased after co-culture for 24, 48, and 72 hours. *$P < 0.05$. ****$P < 0.0001$ by two-tailed t-test. (**D**) MTM cells (*red*) cultured with iPSC-TM for 24 and 48 hours, and treated with DMSO, CBX, or FFA. Typical results from $n = 3$ technical repeats are shown. (**E**) Quantitative analysis of $[Ca^{2+}]_i$ in MTM and iPSC-TM after coculture for 24 and 48 hours in the presence of CBX and FFA. **$P < 0.01$ by 1-way ANOVA. Scale bar = 100 µm. Data shown represent means ± SEM.

$P < 0.001$, $n = 5$; see right panel in Fig. 4B) and a significant elevation of IOP (2 weeks: 15.6 ± 0.4 vs. 13.0 ± 0.4 mm Hg, $P < 0.0001$ $n = 13–14$; 4 weeks: 16.6 ± 0.4 vs. 13.5 ± 0.2 mm Hg, $P < 0.0001$, $n = 13$; 8 weeks: 17.8 ± 0.5 vs. 14.1 ± 0.2 mm Hg, $P < 0.0001$, $n = 6$; Fig. 4C). Several

eyes (10.0%) exhibited severe inflammation due to the infection of adenovirus 5, consistent with previous observations of Ad5 cytotoxicity.[38] These eyes were excluded and only those remaining in good condition are included in the analysis of data. We also noted that EGFP fluorescence, which
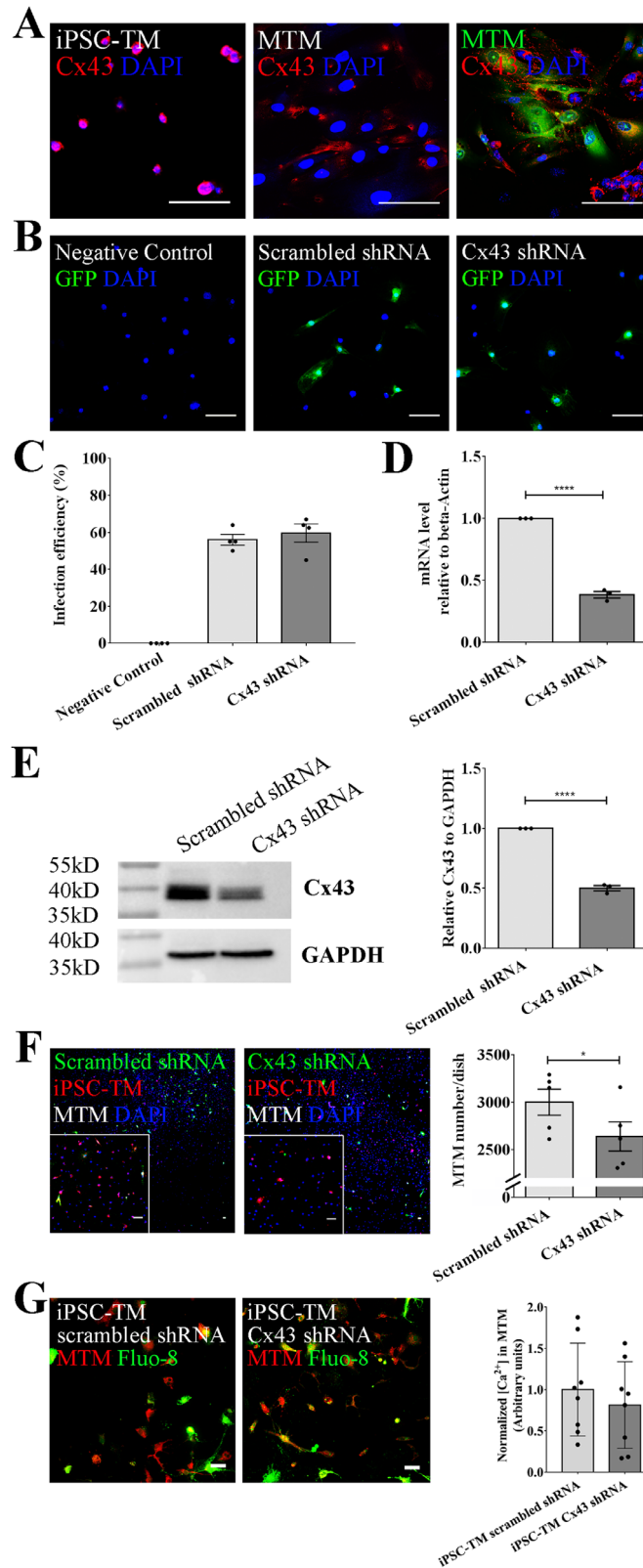
FIGURE 3. Knock-down of Cx43 expression reduces iPSC-TM stimulation of MTM cell division. (A) Immunohistochemical staining of Cx43 (*red*) in iPSC-TM and MTM as well as during coculture when MTM cells are pre-stained with CellTracker Green CMFDA (*green*). (B) Immunohistochemical detection of EGFP indicating lentivirus-infected iPSC-TM cells. Nuclei are labeled with DAPI (*blue*). Typical results from $n = 4$ technical repeats are shown. (C) Infection efficiencies of scrambled shRNA-EGFP lentivirus and Cx43-EGFP lentivirus. (D) Relative mRNA levels of Cx43 after shRNA knock down ($P < 0.0001$, $n = 3$). β-actin is used as the reference gene. (E) *Left panel*: Western blot detection of Cx43 (*top*) or GAPDH (*bottom*) in iPSC-TM transfected with either scrambled shRNA or Cx43 shRNA. Typical results from $n = 3$ technical repeats are shown. *Right panel*: Quantification of band intensities using Image Lab software (Bio-Rad) ($P < 0.0001$).

(**F**) *Left panel*: Immunohistochemical staining of MTM cocultured with iPSC-TM (*green* due shRNA-EGFP transfection; *red* after labeling with CellTracker Red CMTPX) for 48 hours. Nuclei are labeled with DAPI (*blue*). The region in the white frame shows a magnified view. Typical results from $n = 5$ technical repeats are shown. *Right panel*: Quantification indicating that down-regulation of Cx43 leads to a significant decrease of MTM in the coculture system. (**G**) *Left panel*: MTM pre-stained with CellTracker Red CMTPX and iPSC-TM infected with lentivirus expressing Cx43 shRNA-EGFP are co-cultured and stained with Fluo-8 AM. *Right panel*: Quantification indicates that knock down of Cx43 causes a mild decrease of intracellular calcium level in MTM, but statistical significance is not reached. *$P < 0.05$. ****$P < 0.0001$ by two-tailed *t*-test. Scale bar = 100 μm. Data shown represent means ± SEM.

suggests MYOC^{Y437H} expression, diminished after 2 months (see Supplementary Fig. S5). Transplantation of iPSC-TM was thus performed 1 month after Ad5 injection, and its therapeutic effect was monitored for 2 more months (Fig. 5).

Expression of Cx43 in iPSC-TM is Essential for the Restoration of Glaucomatous TM

To avoid the tumorigenicity of residual undifferentiated iPSCs within the iPSC-TM population, we performed a magnetic bead-based approach to remove cells remaining immunopositive for the stem cell marker SSEA-1. Following purification, the fraction of SSEA-1-negative iPSC-TM cells was quantified by flow cytometry. Here, purification resulted in 97.6% SSEA-1 negative cells (see Fig. 5A), which, based upon our experience, is sufficient to avoid teratoma formation.[9,10,13] Purified iPSC-TM were then transfected with lentivirus expressing either scrambled shRNA or Cx43 shRNA, as described above (see Fig. 3) and intracamerally injected into the eyes C57BL/6 mice after induction of elevated IOP, as described above ($n = 18$ of each group). Mice with elevated IOP but having received an injection of PBS instead of iPSC-TM ($n = 10$) and age-matched C57BL/6 mice without elevated IOP receiving PBS injections ($n = 10$) were added as positive and negative controls. In all groups, eyes with severe inflammation were excluded from analysis. We then determined the number of iPSC-TM and endogenous TM cells in the region between the pigmented ciliary body and Schlemm's canal in these eyes. Transplanted iPSC-TM can be discriminated based upon their dsRed fluorescence following signal amplification through labeling with dsRed antibody in vitro (see Fig. 5B) and in vivo (see Figs. 5C, 5D). As observed in our previous studies,[9,10,13] quantification of iPSC-TM implanted into the tissue 51 days after transplantation revealed that only a small number of these cells survive. However, a significant difference between iPSC-TM having received Cx43 shRNA or scrambled shRNA was not noted (0.3 ± 0.1 vs. 0.6 ± 0.2 cells/section, $P = 0.17$, $n = 13$; see Fig. 5D).

Subsequent quantification of overall TM cell density indicated that transplantation of iPSC-TM cells expressing scrambled shRNA significantly increases the overall number of TM cells in Ad5-MYOC^{Y437H}-EGFP mice when compared to the PBS control group (35.8 ± 1.8 vs. 23.6 ± 1.0 cells/section, $P < 0.001$, $n = 6$–15; see Fig. 5D). Downregulation of Cx43 by shRNA in iPSC-TM caused a dramatic decrease in TM cell density when compared to the scrambled shRNA group (28.1 ± 1.3 vs. 35.8 ± 1.8 cells/section, $P < 0.01$, $n = 14$–15; see Fig. 5D). These findings are consistent with previous data demonstrating a TM cell proliferation inducing effect of iPSC-TM transplantation and furthermore indicate that Cx43 plays an important role in this process both in vitro (see Fig. 3) and in vivo (see Fig. 5).

We were particularly interested to determine whether downregulation of Cx43 weakens the regenerative capacity of iPSC-TM in vivo. In this Ad5-MYOC^{Y437H}-EGFP induced glaucoma model, transplantation of iPSC-TM expressing scrambled shRNA resulted in a significant reduction of IOP when compared to the PBS group 26 days after transplantation (15.8 ± 0.2 vs. 17.9 ± 0.2 mm Hg, $P < 0.01$, $n = 10$–18), which was sustained until the termination of the experiment on day 51 (15.3 ± 0.3 vs. 18.4 ± 0.5 mm Hg, $P < 0.0001$, $n = 8$–16; Fig. 5E). In contrast, transplantation of iPSC-TM with reduced Cx43 expression did not lead to a significant reduction of IOP in Ad5-MYOC^{Y437H}-EGFP mice until day 40 and IOP remained significantly above that of mice transplanted with scrambled shRNA treated iPSC-TM (16.5 ± 0.4 vs. 18.7 ± 0.5 mm Hg, $P = 0.02$, $n = 8$–11; see Fig. 5E).

DISCUSSION

The TM cells fulfill a crucial role in the regulation of conventional AH outflow and restoration of TM cell function by stem cells may be a feasible approach to achieve long term AH control outflow and IOP homeostasis in glaucoma.[9,10] The iPSCs are of particular interest for clinical use because their autologous derivation minimizes the potential for graft rejection and poses few ethical issues.[39] A number of studies have demonstrated the high potential of iPSC in regenerative medicine, but how iPSC-based therapy regenerates the TM in glaucoma remains elusive.

We previously demonstrated that iPSC-derived TM cells are not only capable of rebuilding the damaged TM cells in several mouse models of glaucoma, but can also improve AH outflow in aged human donor eyes.[9,10,13,30] We initially assumed that transplanted iPSC-TM would establish themselves in the recipients' TM cells and carry out the functions of endogenous TM cells lost due to the pathophysiologic events of glaucoma. It has become increasingly apparent that this is not the case and that long-term survival of iPSC-TM is rare. Rather, it appears that iPSC-TM transplantation causes proliferation of the remaining endogenous TM cells that then act to restore AH outflow dynamics.[9,10]

In this study, we first established a coculture system to mimic the interaction between iPSC-TM and MTM in vivo. Analogous to our previous findings using primary human iPSC, coculture of MTM and mouse iPSC-TM caused increased proliferation rates of MTM cells, suggesting that transplantation of mouse iPSC-TM has the capacity to increase the population of endogenous TM cells in vivo.

We previously observed that cell culture medium conditioned by iPSC-TM does not stimulate MTM division[13] and that direct cell-cell contact plays an essential role in this process. Communication between neighboring TM cells may involve a number of mechanisms, including tight junctions, anchor junctions, gap junctions, and nanotubes.[40–43] Based upon their prominent expression by TM cells, we sought to investigate whether gap junctions, especially those containing Cx43, are involved. We initially used two selective antagonists for inhibition of gap junction activity, CBX and FFA, and observed a significant reduction of iPSC-TM induced
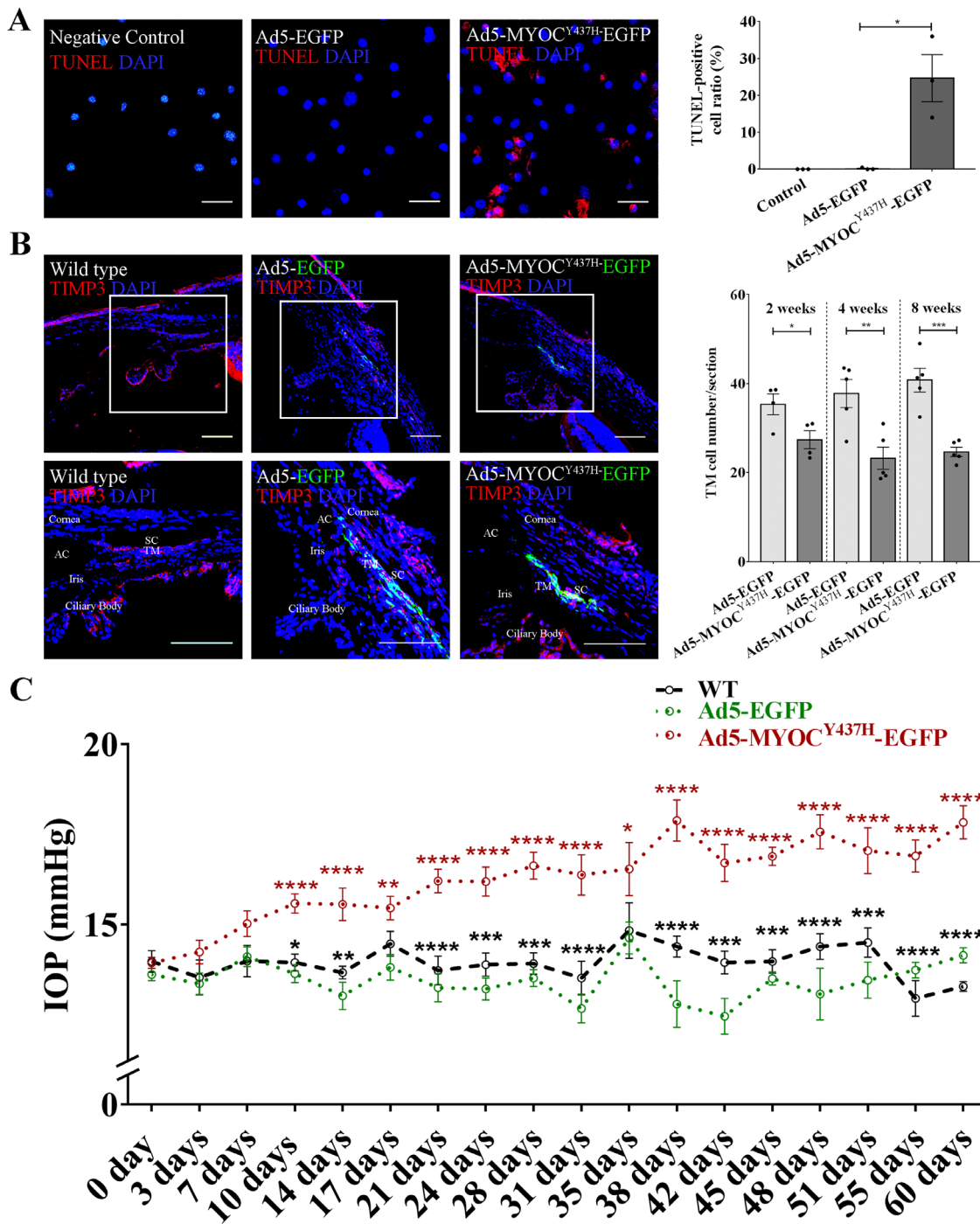
Figure 4. **Expression of MYOC^{Y437H} causes reduction of TM cellularity and IOP elevation in vivo.** (**A**) *Left panel*: Immunohistochemical detection of apoptotic cells (*red*) by TdT-mediated dUTP Nick-End Labeling (TUNEL). Nuclei are labeled with DAPI (*blue*). Typical results from $n = 3$ technical repeats are shown. *Right panel*: Ratio of TUNEL positive MTM cells following infection with Ad5.MYOC^{Y437H}-EGFP. *$P < 0.05$ by two-tailed *t*-test. (**B**) *Left panels*: Immunohistochemical detection of EGFP (*green*) in the TM of 2-month-old C57BL/6 mice 2 weeks after receiving PBS, Ad5.EGFP, and Ad5.MYOC^{Y437H}-EGFP. Immunohistochemical detection of TIMP3 (*red*) for is included to outline the TM. *Right panel*: Quantification of MTM cells in mice 2 weeks ($n = 4$), 4 weeks ($n = 5$), and 8 weeks ($n = 5$) after infection with Ad5.MYOC^{Y437H}-EGFP or Ad5.EGFP. *$P < 0.05$, **$P < 0.01$, ***$P < 0.001$ by two-tailed *t*-test. (**C**) IOP in C57BL/6 mice following injection of PBS ($n = 6$), Ad5.EGFP ($n = 6$–17), or Ad5.MYOC^{Y437H}-EGFP ($n = 6$–17). *$P < 0.05$, **$P < 0.01$, ***$P < 0.001$, ****$P < 0.0001$ by 2-way ANOVA (*red asterisks*: Ad5-MYOC^{Y437H}-EGFP vs. Ad5-EGFP; *black asterisks*: Ad5-MYOC^{Y437H}-EGFP vs. WT). Scale bar = 100 µm. Data shown represent means ± SEM.

MTM division. Although effective, these inhibitors can affect several channels, including those comprised of pannexins,[44] calcium and chloride channels,[45,46] and other transporters.[47]

More definitive proof of the involvement of gap junctions in iPSC-TM induced stimulation of MTM division can be achieved by the targeted removal of specific gap junction
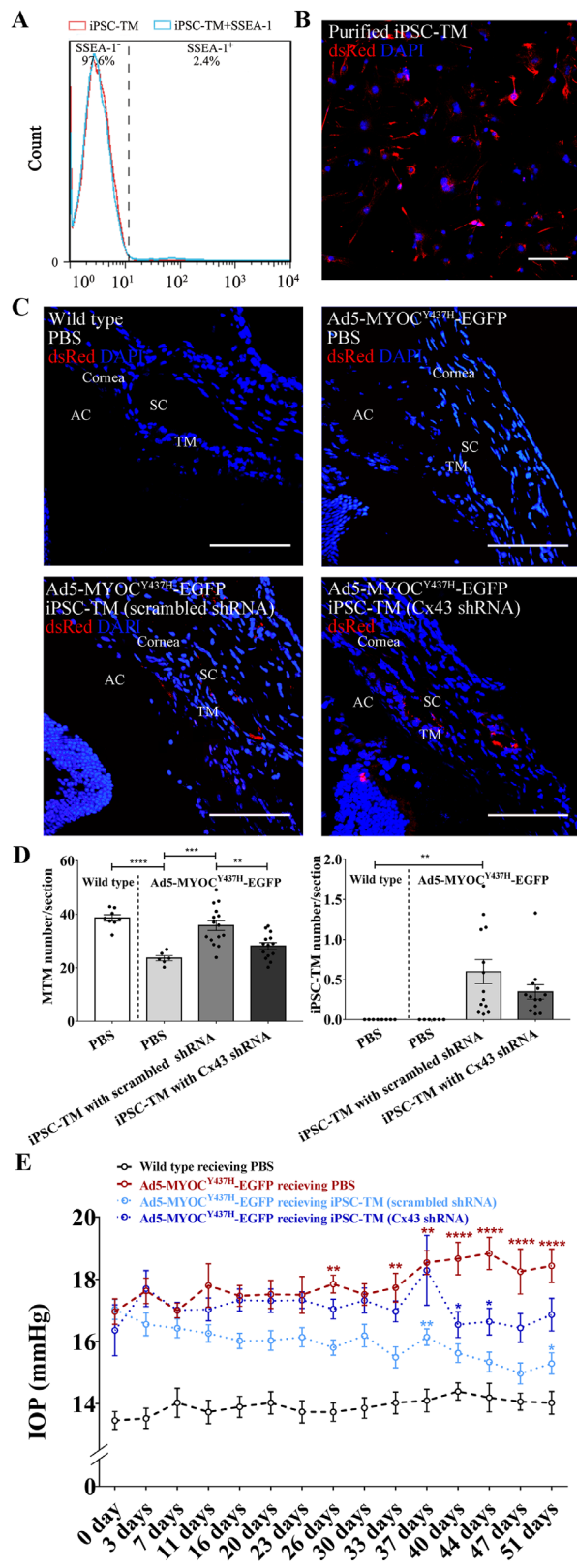
FIGURE 5. **Cx43 is essential for iPSC-TM stimulation of endogenous TM cell division and to restore IOP homeostasis.** (**A**) Detection of iPSC-TM purification rate by flow cytometry. Preparation containing less than 2.4% SSEA-1 positive cells were used for transplantation. (**B**) Immunohistochemical staining of dsRed (*red*) and nuclei (DAPI; *blue*) in purified iPSC-TM cells. Typical results from *n* = 3 technical repeats are shown. (**C**) Immunohistochemical detec-

proteins. Therefore, we used shRNA mediated knockdown of Cx43, which is prominently expressed by TM cells, to determine if this protein plays a crucial role. Although only a partial reduction of Cx43 was achieved by this approach, we nevertheless observed a significant decline in iPSC-TM stimulated MTM cells division, confirming that communication via gap-junctions containing Cx43 occurs between iPSC-TM and primary TM cells and that this process is important in the observed proliferation response by TM cells.

Gap junctions only allow transfer of small molecules (less than 1.2 kD) between neighboring cells and are crucial for transfer of calcium, which frequently acts as a second messenger molecule.[48–50,63] This appears to be also the case here and our data not only demonstrate the transfer of Ca^{2+}, and indicated a significant increase of $[Ca^{2+}]_i$ in MTM and a decrease of $[Ca^{2+}]_i$ in iPSC-TM after coculture. Calcium has been reported to be an essential signal for the regulation of the cell cycle[51–53] and consequently it is possible that the observed calcium influx directly serves to increase MTM cell division. However, the influx of calcium through Cx43 containing gap junctions appears to be mild, which makes it possible that this initial mild calcium influx serves to initiate down-stream responses that then cause a significant increase of calcium concentration in MTM cells.

We next extend our study to investigate the role of Cx43 in the regeneration of TM function using an in vivo mouse model of glaucoma. A number of investigations have demonstrated that mutations in myocilin (MYOC) cause the protein to misfold and aggregate in the endoplasmic reticulum, eventually leading to the death of TM cells.[11,54,55] We, therefore, generated a recombinant Ad5 expressing human MYOC[Y437H] that caused severe loss of TM cells both in vitro and in vivo.[62] Injection of this vector (Ad5.MYOC[Y437H]-EGFP) into the anterior chamber of mice caused robust elevation of IOP lasting until the end of the experiment (80 days). At this point, very little expression of the vector was observed, which may be due to the death of transfected cells or, perhaps, epigenetic silencing of the viral construct. Taken together, the loss of TM cells and the extended duration of elevated IOP indicated that this glaucoma model is feasible for evaluating the effects of cell-based therapies.

tion of dsRed (*red*) and nuclei (DAPI; *blue*) in TM sections mice 51 days after transplantation. Mice received an injection of either PBS (WT, *n* = 8) or Ad5.MYOC[Y437H]-EGFP to elevate IOP. Mice that received adenoviral injections further received sham treatment (PBS, *n* = 6), iPSC-TM expressing scrambled shRNA (*n* = 13–15), or iPSC-TM expressing Cx43 shRNA (*n* = 13–14). (**D**) *Left panel*: Quantitation of MTM in the TM of mice having received an injection of either PBS or Ad5.MYOC[Y437H]-EGFP to elevate IOP. Mice that received adenoviral injections further received sham treatment (PBS, *n* = 6), iPSC-TM expressing scrambled shRNA (*n* = 15), or iPSC-TM expressing Cx43 shRNA (*n* = 14). *Right panel*: Remaining iPSC-TM in iPSC-TM recipients 51 days after transplantation (*n* = 13). No significant difference was observed in mice receiving normal iPSC-TM or modified iPSC-TM (p = 0.17). **$P < 0.01$, ***$P < 0.001$ by 1-way ANOVA. (**E**) IOP measurement in C57BL/6 mice receiving PBS (*n* = 10) and Ad5-MYOC[Y437H]-EGFP. Vector treated mice subsequently receiving injections of PBS (*n* = 8–10), iPSC-TM expressing scrambled shRNA (*n* = 16–18) or iPSC-TM expressing Cx43 shRNA (*n* = 11–18). *$P < 0.05$, **$P < 0.01$, ****$P < 0.0001$ by 2-way ANOVA (*red asterisks*: scrambled shRNA iPSC-TM recipients vs. PBS recipients; *dark blue asterisks*: Cx43 shRNA iPSC-TM vs. PBS recipients; *light blue asterisks*: scrambled shRNA iPSC-TM recipients vs. Cx43 shRNA iPSC-TM). Scale bar = 100 µm. Data shown represent means ± SEM.

We used this mouse model to investigate whether Cx43 is required for the iPSC-TM mediated restoration of TM function. Transplantation of iPSC expressing scrambled shRNA into the anterior chamber of Ad5.MYOC^{Y437H}-EGFP mice resulted in increased TM cellularity and a decrease in IOP that became statistically significant when compared to animals that did not receive iPSC-TM 28 days after transplantation. In contrast, transplantation of iPSC-TM modified to express Cx43 shRNA did not result in a significant increase of TM cell density. These animals also exhibited a much reduced therapeutic effect. The decline in IOP was less than that in mice having received unmodified iPSC-TM and did not become statistically significant until 40 days after transplantation. Although these findings clearly indicate a significant role for Cx43 gap junction mediated communication between iPSC-TM and TM cells in the proliferative response, the residual activity of the Cx43 shRNA modified iPSC-TM introduces the question whether other cell communication mechanisms, such as nanotubes,[56] may be involved in the observed phenomenon. On the other hand, the knock down of Cx43 was incomplete and 40.4% expression of Cx43 was retained. It is equally possible that this residual activity is sufficient to eventually cause a reversal of elevated IOP. It would be of particular interest to examine the role of iPSC-TM after the complete knockout of Cx43.

Despite the regenerative effect of transplantation, the number of iPSC-TM cells retained in the TM after transplantation is very limited. Only 0.3 to 0.6 dsRed positive cells were detected in each section 51 days after transplantation, although implanted cells were detected at a higher frequency 1 day after transplantation (Supplementary Fig. S7). These findings are also in agreement with our previous studies that indicated that transplanted iPSC-TM cells integrate into the TM immediately after transplantation, but their numbers gradually diminish.[13] These data indicate that transplanted iPSC-TM cells do not survive well in the eyes, regardless of their expression of Cx43 or not, but also that long-term survival is not required for a therapeutic effect. This observation is very different from those reported in studies using TM stem cells that have a strong capacity to anchor and integrate into the TM for an extended period after transplantation.[31,39] Likewise, mesenchymal stem cells that may regenerate the TM through its paracrine capacity[57] appear to survive in the TM for many days.

In this study, transplantation of iPSC-TM into the eyes of Ad5.MYOC^{Y437H} treated mice proved to be more effective than previously observed in transgenic MYOC^{Y437H} mice, despite the fact that the same number of cells was transplanted. Here, a significant IOP reduction was apparent in individual mice as early as 11 days after transplantation and IOP changes in the whole group of treated mice became statistically significant on day 26. This contrasts with our earlier studies where a significant IOP reduction was not achieved until 42 days after transplantation and even longer. The reason for this divergence is currently unclear but could be due to several factors. Batch to batch differences may occur during the induction of iPSC-TM and is conceivable that the cells generated for this study are more potent with respect to the induction of TM cell proliferation than those used in earlier studies.

Another possibility is that the observed disparities are due to differences in the mouse models used. Although both models are based upon expression of MYOC^{Y437H}, Ad5 mediated transfection likely only affects a subset of TM cells, whereas this pathogenic variant is expressed in all TM cells in transgenic animals, including those resulting from iPSC-TM induced TM cell proliferation. This may result in less pronounced TM damage in Ad5.MYOC^{Y437H} mice that is more amenable to restoration. It must also be pointed out that in our hands Tg-MYOC^{Y437H} mice on a C57BL/6 genetic background rarely develop significantly elevated IOP and experimental animals are all generated on a mixed C57BL/6 and SJL background. Whereas application of the Ad5.MYOC^{Y437H} vector reliably causes TM dysfunction and IOP elevation in C57BL/6 mice, it is nevertheless conceivable that the genetic makeup of this strain benefits TM cell survival and tissue regeneration.

It is also possible that the observed differences are related to the fact that the Ad5-MYOC^{Y437H} mice used in this study are younger than the Tg-MYOC^{Y437H} animals used previously. We previously demonstrated that restoration of normal IOP following iPSC-TM transplantation occurs more rapidly in 4 month old Tg-MYOC^{Y437H} mice than in 6 month old animals.[9,10] Consequently the 3 month old mice used in this study may exhibit an even greater regenerative ability. Delayed resolution of elevated IOP in older mice may be the result of accumulating TM damage that is more difficult to reverse, but could also be due to reduced viability in older cells when compared to those from younger animals.[58–60] Although cell senescence induced by passaging differs in some respects from physiological senescence,[61] the notion that TM cells in younger mice divide more readily than in older animals is in agreement with our observation that the efficiency of iPSC-TM to stimulate cell division is reduced in MTM at higher passages.

In summary, our results establish a role of gap junction in iPSC-TM stimulated MTM division. Cx43 is widely expressed in both iPSC-TM and MTM cells, and appears to carry an important function in this process. Knock down of Cx43 expression blunts the regenerative ability of iPSC-TM cells to enhance MTM cell division and prevents the restoration of disrupted IOP homeostasis in glaucoma. These data provide a first mechanistic insight into the cellular events associated with TM restoration resulting from iPSC-TM transplantation.

References

1. Quigley HA. Glaucoma. *Lancet (London, England)*. 2011; 377:1367–1377.
2. Quigley HA, Broman AT. The number of people with glaucoma worldwide in 2010 and 2020. *Br J Ophthalmol*. 2006;90:262–267.
3. Carreon T, van der Merwe E, Fellman RL, Johnstone M, Bhattacharya SK. Aqueous outflow - A continuum from

trabecular meshwork to episcleral veins. *Prog Retinal Eye Res*. 2017;57:108–133.

4. Grant WM. Experimental aqueous perfusion in enucleated human eyes. *Arch Ophthalmol (Chicago, Ill: 1960)*. 1963;69:783–801.

5. Zhou Y, Xia X, Yang E, et al. Adipose-derived stem cells integrate into trabecular meshwork with glaucoma treatment potential. *FASEB J*. 2020;34:7160–7177.

6. Du Y, Yun H, Yang E, Schuman JS. Stem cells from trabecular meshwork home to TM tissue in vivo. *Invest Ophthalmol Vis Sci*. 2013;54:1450–1459.

7. Yun H, Wang Y, Zhou Y, et al. Human stem cells home to and repair laser-damaged trabecular meshwork in a mouse model. *Commun Biol*. 2018;1:216.

8. Manuguerra-Gagné R, Boulos PR, Ammar A, et al. Transplantation of mesenchymal stem cells promotes tissue regeneration in a glaucoma model through laser-induced paracrine factor secretion and progenitor cell recruitment. *Stem Cells (Dayton, Ohio)*. 2013;31:1136–1148.

9. Zhu W, Gramlich OW, Laboissonniere L, et al. Transplantation of iPSC-derived TM cells rescues glaucoma phenotypes in vivo. *Proc Natl Acad Sci USA*. 2016;113:E3492–E500.

10. Zhu W, Jain A, Gramlich OW, Tucker BA, Sheffield VC, Kuehn MH. Restoration of Aqueous Humor Outflow Following Transplantation of iPSC-Derived Trabecular Meshwork Cells in a Transgenic Mouse Model of Glaucoma. *Invest Ophthalmol Vis Sci*. 2017;58:2054–2062.

11. Joe MK, Sohn S, Hur W, Moon Y, Choi YR, Kee C. Accumulation of mutant myocilins in ER leads to ER stress and potential cytotoxicity in human trabecular meshwork cells. *Biochem Biophys Res Commun*. 2003;312:592–600.

12. Zode GS, Kuehn MH, Nishimura DY, et al. Reduction of ER stress via a chemical chaperone prevents disease phenotypes in a mouse model of primary open angle glaucoma. *J Clin Invest*. 2015;125:3303.

13. Zhu W, Godwin CR, Cheng L, Scheetz TE, Kuehn MH. Transplantation of iPSC-TM stimulates division of trabecular meshwork cells in human eyes. *Sci Rep*. 2020;10:2905.

14. Goodenough DA, Goliger JA, Paul DL. Connexins, connexons, and intercellular communication. *Ann Rev Biochem*. 1996;65:475–502.

15. Evans WH, Martin PE. Gap junctions: structure and function (Review). *Mol Membr Biol*. 2002;19:121–136.

16. Kerr NM, Johnson CS, Green CR, HV Danesh-Meyer. Gap junction protein connexin43 (GJA1) in the human glaucomatous optic nerve head and retina. *J Clin Neurosci*. 2011;18:102–108.

17. Zong L, Zhu Y, Liang R, Zhao HB. Gap junction mediated miRNA intercellular transfer and gene regulation: A novel mechanism for intercellular genetic communication. *Sci Rep*. 2016;6:19884.

18. Dominique T, Eric S, Carmen G. The Microvascular Gap Junction Channel: A Route to Deliver MicroRNAs for Neurological Disease Treatment. *Front Mol Neurosci*. 2017;10:246.

19. Fan X, Teng Y, Ye Z, Zhou Y, Tan WS. Gap junction-mediated MiR-200b on osteogenesis and angiogenesis in coculture between MSCs and HUVECs. *J Cell Sci*. 2018;131: jcs216135.

20. Ding QJ, Zhu W, Cook AC, Anfinson KR, Tucker BA, Kuehn MH. Induction of trabecular meshwork cells from induced pluripotent stem cells. *Invest Ophthalmol Vis Sci*. 2014;55:7065–7072.

21. Yu H, Miao Y, Chen W, et al. Expressional and functional involvement of gap junctions in aqueous humor outflow into the ocular trabecular meshwork of the anterior chamber. *Mol Vis*. 2019;25:255–265.

22. Mao W, Liu Y, Wordinger RJ, Clark AF. A magnetic bead-based method for mouse trabecular meshwork cell isolation. *Invest Ophthalmol Vis Sci*. 2013;54:3600–3606.

23. Min HK, Rhee DJ. Suppression of thrombospondin-1 (TSP1) in Human Trabecular Meshwork Alters Extracellular Matrix. *Invest Ophthalmol Vis Sci*. ARVO Annual Meeting Abstract, September 2016. Available at: https://iovs.arvojournals.org/article.aspx?articleid=2557671.

24. Shepard AR, Jacobson N, Millar JC, et al. Glaucoma-causing myocilin mutants require the Peroxisomal targeting signal-1 receptor (PTS1R) to elevate intraocular pressure. *Hum Mol Genet*. 2007;16:609–617.

25. Hernandez H, Millar JC, Curry SM, Clark AF, McDowell CM. BMP and Activin Membrane Bound Inhibitor Regulates the Extracellular Matrix in the Trabecular Meshwork. *Invest Ophthalmol Vis Sci*. 2018;59:2154–2166.

26. Arora AI, Johar K, Gajjar DU, et al. Cx43, ZO-1, alpha-catenin and beta-catenin in cataractous lens epithelial cells. *J Bioscie*. 2012;37:979–987.

27. Zode GS, Kuehn MH, Nishimura DY, et al. Reduction of ER stress via a chemical chaperone prevents disease phenotypes in a mouse model of primary open angle glaucoma. *J Clin Invest*. 2011;121:3542–3553.

28. Zhu W, Hou F, Fang J, et al. The role of Piezo1 in conventional aqueous humor outflow dynamics. *iScience*. 2021;24:102042.

29. Keller KE, Bhattacharya SK, Borrás T, et al. Consensus recommendations for trabecular meshwork cell isolation, characterization and culture. *Exp Eye Res*. 2018;171:164–173.

30. Cheng L, Zhu W, Wareham LK, Buys ES, Kuehn MH. Trabecular meshwork restoration in primary open-angle glaucoma using stem cells. In: *Glaucoma Research 2020-2022* (pp. 29–40). Amsterdam: Kugler Publications; 2020.

31. Xiong S, Kumar A, Tian S, et al. Stem cell transplantation rescued a primary open-angle glaucoma mouse model. *eLife*. 2021;10:e63677.

32. Yin X, Feng L, Ma D, et al. Roles of astrocytic connexin-43, hemichannels, and gap junctions in oxygen-glucose deprivation/reperfusion injury induced neuroinflammation and the possible regulatory mechanisms of salvianolic acid B and carbenoxolone. *J Neuroinflam*. 2018;15:97.

33. Ruan Z, Orozco IJ, Du J, Lü W. Structures of human pannexin 1 reveal ion pathways and mechanism of gating. *Nature*. 2020;584:646–651.

34. Calder BW, Matthew Rhett J, Bainbridge H, Fann SA, Gourdie RG, Yost MJ. Inhibition of connexin 43 hemichannel-mediated ATP release attenuates early inflammation during the foreign body response. *Tissue Eng Part A*. 2015;21:1752–1762.

35. Verselis VK, Srinivas M. Connexin channel modulators and their mechanisms of action. *Neuropharmacology*. 2013;75:517–524.

36. Guinamard R, Simard C, Del Negro C. Flufenamic acid as an ion channel modulator. *Pharmacol Ther*. 2013;138:272–284.

37. Tsui E, Hill KA, Laliberte AM, Paluzzi D, Hutnik CML. Ocular pathology relevant to glaucoma in a Gja1(Jrt/+) mouse model of human oculodentodigital dysplasia. *Invest Ophthalmol Vis Sci*. 2011;52:3539–3547.

38. Catalucci D, Sporeno E, Cirillo A, Ciliberto G, Nicosia A, Colloca S. An adenovirus type 5 (Ad5) amplicon-based packaging cell line for production of high-capacity helper-independent deltaE1-E2-E3-E4 Ad5 vectors. *J Virol*. 2005;79:6400–6409.

39. Volarevic V, Markovic BS, Gazdic M, et al. Ethical and Safety Issues of Stem Cell-Based Therapy. *Int J Med Sci*. 2018;15:36–45.

40. Russ PK, Kupperman AI, Presley SH, Haselton FR, Chang MS. Inhibition of RhoA signaling with increased Bves in trabecular meshwork cells. *Invest Ophthalmol Vis Sci*. 2010;51:223–230.

41. Tanino T, Hida T, Azuma N. [Histochemical and electron microscopic study of the formation of trabecular meshwork

and changes of glycosaminoglycans]. *Nippon Ganka Gakkai Zasshi*. 1993;97:310–317.

42. Kimura S, Suzuki K, Sagara T, Nishida T, Yamamoto T, Kitazawa Y. Regulation of connexin phosphorylation and cell-cell coupling in trabecular meshwork cells. *Invest Ophthalmol Vis Sci*. 2000;41:2222–2228.

43. Angulo-Urarte A, van der Wal T, Huveneers S. Cell-cell junctions as sensors and transducers of mechanical forces. *Biochim Biophys Acta Biomembr*. 2020;1862: 183316.

44. Bruzzone R, Barbe MT, Jakob NJ, Monyer H. Pharmacological properties of homomeric and heteromeric pannexin hemichannels expressed in Xenopus oocytes. *J Neurochem*. 2005;92:1033–1043.

45. Ye ZC, Wyeth MS, Baltan-Tekkok S, Ransom BR. Functional hemichannels in astrocytes: a novel mechanism of glutamate release. *J Neurosci*. 2003;23:3588–3596.

46. Hongxia Yongzhen, Miao , et al. Expressional and functional involvement of gap junctions in aqueous humor outflow into the ocular trabecular meshwork of the anterior chamber. *Mol Vis*. 2019;25:255–265.

47. Dahl G, Qiu F, Wang J. The bizarre pharmacology of the ATP release channel pannexin1. *Neuropharmacology*. 2013;75:583–593.

48. Willebrords J, Crespo Yanguas S, Maes M, et al. Structure, Regulation and Function of Gap Junctions in Liver. *Cell Commun Adhes*. 2015;22:29–37.

49. Das PN, Mehrotra P, Mishra A, Bairagi N, Chatterjee S. Calcium dynamics in cardiac excitatory and non-excitatory cells and the role of gap junction. *Math Biosci*. 2017;289:51–68.

50. Parys B, Côté A, Gallo V, De Koninck P, Sík A. Intercellular calcium signaling between astrocytes and oligodendrocytes via gap junctions in culture. *Neuroscience*. 2010;167:1032–1043.

51. Peracchia C. Calmodulin-Mediated Regulation of Gap Junction Channels. *Int J Mol Sci*. 2020;21:485.

52. Schumacher JA, Hsieh YW, Chen S, et al. Intercellular calcium signaling in a gap junction-coupled cell network establishes asymmetric neuronal fates in C. elegans. *Development (Cambridge, England)*. 2012;139:4191–4201.

53. Pearson RA, Catsicas M, Becker DL, Bayley P, Lüneborg NL, Mobbs P. Ca(2+) signalling and gap junction coupling within and between pigment epithelium and neural retina in the developing chick. *Eur J Neurosci*. 2004;19:2435–2445.

54. Zillig M, Wurm A, Grehn FJ, Russell P, Tamm ER. Overexpression and properties of wild-type and Tyr437His mutated myocilin in the eyes of transgenic mice. *Invest Ophthalmol Vis Sci*. 2005;46:223–234.

55. Jacobson N, Andrews M, Shepard AR, et al. Non-secretion of mutant proteins of the glaucoma gene myocilin in cultured trabecular meshwork cells and in aqueous humor. *Hum Mol Genet*. 2001;10:117–125.

56. Li X, Acott TS, Nagy JI, Kelley MJ. ZO-1 associates with α3 integrin and connexin43 in trabecular meshwork and Schlemm's canal cells. *Int J Physiol Pathophysiol Pharmacol*. 2020;12:1–10.

57. Stern JH, Tian Y, Funderburgh J, et al. Regenerating Eye Tissues to Preserve and Restore Vision. *Cell Stem Cell*. 2018;22:834–849.

58. Wu Q, Zhan J, Pu S, Qin L, Li Y, Zhou Z. Influence of aging on the activity of mice Sca-1+CD31- cardiac stem cells. *Oncotarget*. 2017;8:29–41.

59. Kretlow JD, Jin YQ, Liu W, et al. Donor age and cell passage affects differentiation potential of murine bone marrow-derived stem cells. *BMC Cell Biol*. 2008;9:60.

60. Azuma E, Hirayama M, Yamamoto H, Komada Y. The role of donor age in naive T-cell recovery following allogeneic hematopoietic stem cell transplantation: the younger the better. *Leuk Lymphoma*. 2002;43:735–739.

61. Gruber HE, Somayaji S, Riley F, et al. Human adipose-derived mesenchymal stem cells: serial passaging, doubling time and cell senescence. *Biotech Histochem*. 2012;87:303–311.

62. Kahraman S, Dirice E, Sanlioglu AD, et al. In vivo fluorescence imaging is well-suited for the monitoring of adenovirus directed transgene expression in living organisms. *Molec Imag Biol*. 2010;12:278–285.

63. Liu Y, Liu Z, Wang KW. The Ca^{2+}-activated chloride channel ANO1/TMEM16A: An emerging therapeutic target for epithelium-originated diseases? *Acta Pharm Sin B*. 2021;11(6):1412–1433, doi:10.1016/j.apsb.2020.12.003.